

## Response to Referee #1

**Manuscript Reference Number: nhess-2014-263**

Manuscript title: Debris flows in the Eastern Italian Alps: seasonality and atmospheric circulation patterns

by

E. I. Nikolopoulos, M. Borga, F. Marra, S. Crema, L. Marchi

We would like to thank the reviewer for their constructive comments. We have revised the manuscript according to these comments and below we provide our detailed response to the points raised by the reviewer. Comments from the reviewer are in black and our response in color.

Note also that corresponding changes in manuscript have been highlighted in the revised version of the manuscript (following after the end of our response).

The manuscript of Nikolopoulos and co-authors entitled “Debris flows in the Eastern Italian Alps: seasonality and atmospheric circulation patterns” is an interesting well-structured manuscript combining correctly the climate data with the debris flow system. The paper addresses relevant scientific and technical questions which are within the scope of NHESS.

Response

Thank you

General comments

1. Authors conclude that Debris flows events during the summer are associated with lower rainfall accumulation and shorter duration while during the fall DF events are characterized by higher accumulations and longer durations. However, no physical explanation on the hydrologic system is proposed to justify such behavior.

Response

We would like to thank the reviewer for highlighting this point. The seasonal characteristics of debris flow triggering rainfall events reflect the general seasonal characteristics of rainfall in the region. Namely, short duration convective systems dominate summer rainfall while long duration widespread systems are typically

dominating rainfall regime during fall. This is now better clarified in conclusions by revising concluding statement as follows:

*Rainfall properties (accumulation and duration) derived for each individual debris flow location and from the closest available raingauge, exhibit a seasonal pattern as well. On average, summer events are associated with lower rainfall accumulation and shorter duration than fall events but with higher intensity. Essentially, this is a reflection of the general seasonal characteristics of rainfall in the region, where rainfall during summer is dominated by short duration convective systems, while during fall season widespread long-lived systems prevail (Borga et al., 2005).*

2. The section 3.4 is devoted to the DF rainfall thresholds. The intensity–duration (ID) threshold was applied to different season and weather circulation type. However, the evaluation of false positives is missing and should be considered to improve the overall quality of the paper.

#### Response

We understand the point raised by the reviewer. However, we need to note that evaluation of the efficiency of ID thresholds as predictors is not the focus of this study. In addition, potential evaluation of the effectiveness of ID thresholds becomes particularly difficult when it comes to evaluation of “false positives” because a debris flow event not in record does not necessarily means that it did not occur. It can also be reminded that rainfall thresholds can be exceeded by rainstorm that do not trigger debris flows in a given catchment because of the (temporary) absence of debris prone to mobilization. Focusing on this intrinsic limitation of rainfall-based debris flow prediction would add little information to the analysis proposed in this paper. The main goal of this work is to analyze the seasonal and weather type dependence of debris flow events in the area of study. Reference to ID thresholds (i.e. section 3.4) aims primarily in demonstrating how the dependencies found for DF rainfall translate in dependencies of ID thresholds. We believe that the later is clearly shown from current analysis and highlights an issue with practical merit. Therefore we would like to maintain section 3.4 focused on presenting only the variability of ID thresholds according to seasonal/weather type characteristics.

#### Particular remarks

3. Page 7198, line 1-2 “The work examines the seasonality and large-scale atmospheric circulation patterns associated to debris flows occurrence”, instead of “The work examines the seasonality and large-scale atmospheric circulation patterns of debris flows”

Response  
Corrected

4. Page 7203, lines 8-9 “DF occurrence is dominated by long duration ( $> 24$  h) events which account for 82% of the DF occurrences”. Authors should specify the long duration concept (up to XX h).

#### Response

We are considering rainfall events that last more than 1 day as long duration events. However, we understand that this holds a degree of subjectivity and may contradict others perception. Therefore we have revised the sentence as follows to avoid potential confusion:

*DF occurrence is dominated by events with duration  $>24h$ , which account for  $\sim 82\%$  of the DF occurrences*

5. Figure 1 – The grey circles representing debris flows cannot be distinguished on zones with higher elevation.

#### Response

Figure 1 has been revised accordingly to improve presentation quality/clarity.

6. The reviewer would prefer a more formal figure caption for figures 6, 7 and 9.

#### Response

We have revised captions in corresponding figures

1 **Debris flows in the Eastern Italian Alps:**  
2 **seasonality and atmospheric circulation patterns**

3  
4  
5

6 E. I. Nikolopoulos<sup>a,\*</sup>, M. Borga<sup>a</sup>, F. Marra<sup>b</sup>, S. Crema<sup>c</sup>, L. Marchi<sup>c</sup>

7

8 <sup>a</sup> Department of Land, Environment, Agriculture and Forestry, University of Padova,  
9 Legnaro, Italy

10 <sup>b</sup> Department of Geography, Hebrew University of Jerusalem, Israel

11 <sup>c</sup> Consiglio Nazionale delle Ricerche, IRPI, Padova, Italy

12

13

14 \*Corresponding author. Tel: (+39) 0498272681; Fax: (+39) 0498272750

15

16

17 E-mail address: [efthymios.nikolopoulos@unipd.it](mailto:efthymios.nikolopoulos@unipd.it) (E.I. Nikolopoulos)

18

19 **Abstract**

20 The work examines the seasonality and large-scale atmospheric circulation patterns  
21 associated to debris flows occurrence in the Trentino-Alto Adige region (Eastern Italian  
22 Alps). Analysis is based on classification algorithms applied on a uniquely dense archive  
23 of debris flows and hourly rain gauge precipitation series covering the period 2000-2009.  
24 Results highlight the seasonal and synoptic forcing patterns linked to debris flows in the  
25 study area. Summer and fall season account for 92% of the debris flows in the record,  
26 while atmospheric circulation characterized by Zonal West, Mixed and Meridional South,  
27 Southeast patterns account for 80%. Both seasonal and circulation patterns exhibit  
28 geographical preference. In the case of seasonality, there is a strong north-south  
29 separation of summer-fall dominance while spatial distribution of dominant circulation  
30 patterns exhibits clustering, with both Zonal West and Mixed prevailing in the northwest  
31 and central east part of the region, while the southern part relates to Meridional South,  
32 Southeast pattern. Seasonal and synoptic pattern dependence is pronounced also on the  
33 debris flow triggering rainfall properties. Examination of rainfall intensity-duration  
34 thresholds derived for different data classes (according to season and synoptic pattern)  
35 revealed a distinct variability in estimated thresholds. These findings imply a certain  
36 control on debris-flow events and can therefore be used to improve existing alert systems.  
37

# 38 1 Introduction

39 Debris flows are recognized as one of the most devastating natural disasters for  
40 mountainous regions at global scale (Dowling and Santi, 2014). The sudden occurrence  
41 combined with the high destructive power of debris flows pose a significant threat to  
42 human life and infrastructures (Petley, 2012). Therefore, developing early warning  
43 procedures for the mitigation of debris flows risk is of great economical and societal  
44 importance.

45 Effective debris flows warning procedures require accurate knowledge on the relevant  
46 triggering mechanisms and their corresponding characteristics (Borga et al. 2014).  
47 Indisputably, rainfall is the predominant factor controlling debris flow triggering. Hence  
48 most of the work so far on the prediction of debris flow occurrence is focused on the  
49 identification of relevant rainfall conditions (Guzzetti et al. 2008 and references therein;  
50 Nikolopoulos et al., 2014). However, the vast majority of the literature on identification  
51 of debris flow triggering rainfall conditions deals primarily with the estimation of rainfall  
52 properties (e.g. rainfall duration, intensity or accumulation) leading to debris flows. Less  
53 attention has been paid to the seasonal and meteorological characteristics of the triggering  
54 rainfall events. Knowledge on the seasonality and meteorological patterns characterizing  
55 debris flow triggering rainfall events is important for two main reasons. First,  
56 classification of debris flow events according to these factors may be used for the  
57 development of a typology for debris flow rainfall events. This typology can  
58 subsequently be used for refining the rainfall triggering conditions according to different  
59 debris flow types and thus improve prediction. This hypothesis was examined by Govi et  
60 al. (1985) who analyzed the seasonality effect on the triggering of shallow landslides (soil  
61 slip – mud flow and soil slip – debris flow) in a sector of NW Italy. It is also justified  
62 from the recent works of Peruccacci et al. (2012) and Vennari et al. (2014) who  
63 demonstrated differences in debris flow triggering rainfall properties between warm and  
64 cold season for central and southern Italy, respectively. Furthermore, Toreti et al. (2013)  
65 showed that debris flow occurrence in southern Swiss Alps, exhibit a distinct pattern in  
66 large-scale atmospheric circulation and suggested that this information can be used to  
67 improve existing warning systems. On this line, Turkington et al. (2014), in a study

68 centered on the southern French Alps, showed that empirical thresholds can be directly  
69 identified based on regional atmospheric patterns.

70 Second, linking debris flow occurrence with seasonal and meteorological characteristics  
71 may provide indications on the potential impact of climate change on debris flow activity  
72 (Stoffel et al., 2014). As an example, Schneuwly-Bollscheider and Stoffel (2012)  
73 concluded that the observed seasonal shift in debris flow activity in the Zermatt valley  
74 (Switzerland) is attributed to changes in precipitation and temperature regime in Swiss  
75 Alps over the last century.

76 The main objective of this work is to investigate the existence of distinct patterns in  
77 seasonality and large-scale atmospheric circulation associated with rainfall events that  
78 trigger debris flows. Furthermore, examination of debris flow rainfall properties with  
79 respect to seasonality and weather circulation patterns is investigated to evaluate the  
80 potential benefit of using such discriminant factors for the identification of debris flow  
81 triggering rainfall conditions. The work is focused over the region Trentino-Alto Adige in  
82 the eastern Italian Alps and the analysis is based on a 10yrs record of debris flows and  
83 raingauge rainfall observations. Section 2 provides a description of the study area and the  
84 different data sources used in the analysis. Results from the analysis are presented and  
85 discussed in Section 3. The main conclusions derived from this work are summarized in  
86 Section 4.

## 87 **2 Study area and data**

### 88 **2.1 The Trentino-Alto Adige region**

89 The Trentino-Alto Adige study region is located in the Eastern Italian Alps (Fig. 1); it  
90 covers 13,607 km<sup>2</sup> and is characterized by complex topography with elevation ranging  
91 from 65 to almost 4000 m a.s.l. (mean elevation is approximately 1600 m a.s.l.). Mean  
92 annual precipitation amounts exhibit strong spatial variability in the region, with annual  
93 sums of slightly above 500 mm in the north-western portion of the region (the Venosta  
94 Valley, located in the rain-shaded Inner Alps) and exceeding 1500 mm in the south-  
95 eastern edge of the area. The features of the precipitation mean annual climatology

96 exhibit characteristic seasonal variations (Norbiato et al, 2009; Parajka et al., 2010). The  
97 precipitation regime in the northern part of the study area is characterized as continental,  
98 with a unimodal cycle and the highest precipitation amount during the main convective  
99 period (May-September). The southern portion of the study area exhibits a bimodal  
100 regime, with maxima in spring-early summer and in autumn, which generally receives the  
101 most abundant precipitation. Typically the precipitation during cold months (October to  
102 April) is in the form of snow and widespread precipitation while mesoscale convective  
103 systems and localized thunderstorms dominate the precipitation regime during warm  
104 months (May to September) (Norbiato et al. 2009; Mei et al. 2014).

105 There are two important factors that make the area attractive for this study. First, the  
106 region is characterized by significant societal risk due to both the high frequency and the  
107 impact (in terms of casualties) of landslides in the area (Salvati et al. 2010). Second, the  
108 availability of a long-term record of precipitation and debris flows (Nikolopoulos et al.,  
109 2014), as described in detail in the following section.

110

## 111 **2.2 Debris flow and rainfall database**

112 Ten years (2000-2009) of available precipitation observations and debris flow (DF,  
113 hereinafter) records are analyzed in this work. Compilation of the DF events occurred in  
114 the region during the period 2000-2009 was based on two independent databases,  
115 covering the two administrative units: Trentino (377 events) and Alto Adige (444 events).  
116 The selected 821 were identified based on a larger number of events in order to get the  
117 same level of spatial and temporal occurrence accuracy. Available information includes  
118 the location of the individual DF initiation point (shown in Fig.1) with a 500 m spatial  
119 accuracy and the date of occurrence with a daily accuracy. Hourly accumulation values of  
120 precipitation are obtained from a network of 192 rain gauges that cover the study region  
121 (Fig. 1). As can be seen from Fig. 1, rain gauge stations are spread quite uniformly over  
122 the region providing a spatial density approximately equal to 1/80 (station/km<sup>2</sup>). The  
123 average (standard deviation) of Euclidian distance and absolute altitudinal difference  
124 between debris flows and closest available rain gauge is 3.7 (1.9) km and 0.43 (0.41) km  
125 respectively.



## 126 **2.3 Weather circulation patterns**

127 The Hess and Brezowsky Grosswetterlagen (GWL) classification system (Hess and  
128 Brezowsky, 1952, 1969, 1977) is used for the classification of large scale atmospheric  
129 flow and weather circulation patterns. The GWL classification system is based on the  
130 mean air pressure distribution (sea level and 500 hPa level) over the North Atlantic  
131 Ocean and Europe. The classification initially identifies three groups of circulation types  
132 (zonal, mixed and meridional), which are divided into 5 major types, which in turn are  
133 divided into 29 subtypes (*Grosswetterlagen*, GWL) (Gestengabe and Werner, 2005;  
134 James 2007). This classification system is frequently used to characterize the atmospheric  
135 flow and weather patterns over the eastern North Atlantic and Europe (Gestengarbe and  
136 Werner, 2005; Kysel'y and Huth, 2006; Planchon et al., 2009). Following Gestengabe  
137 and Werner (2005) and Parajka et al. (2010), the original GWL classes were further  
138 grouped into six categories (Table 1) that were used for the description of the general  
139 weather regime during DF events. For more detailed information on the GWL  
140 classification system and the individual GWL weather types, the interested reader is  
141 referred to Gestengabe and Werner (2005) and James (2007) and references therein.

142 The monthly frequency of the GWL groups (Table 1) is presented in Fig. 2, for the whole  
143 study period (2000-2009). As it is shown, the occurrence of Mixed weather pattern  
144 dominates the other patterns consistently over all months, with monthly occurrence being  
145 greater than 30% in all cases. On the other hand, the Mixed CE type is associated with  
146 the minimum occurrence (less than 5% for all months except ~10% in August), while the  
147 frequency for the rest of the weather patterns is within the same range and generally  
148 between 10 to 20%. One noticeable feature is that during the winter period, apart from  
149 the Mixed type, the Zonal West pattern occurrence is significant and distinctly higher  
150 than the rest.

# 151 **3 Analysis and results**

## 152 **3.1 Spatial distribution of debris flow triggering rainfall properties**

153 Characteristic properties, namely duration and accumulation, for each DF triggering  
154 rainfall event are estimated from the closest available rain gauge. Calculation of event-

155 based properties is based on the identification of individual events in the rainfall records  
156 by separating subsequent rainfall events according to an inter-event period of 24  
157 consecutive hours without rainfall (Nikolopoulos et al, 2014). This procedure results in  
158 the identification of a total of 128 individual rainfall events, which have triggered the 821  
159 DF analyzed. To examine the spatial distribution of DF rainfall properties, results are  
160 grouped into different classes of duration and accumulation respectively and are mapped  
161 over the study region (Fig. 3). Geographical distribution of the DF rainfall properties, as  
162 shown in Fig. 3, allow us to investigate and potentially identify areas over the study  
163 region with distinct pattern in the characteristics of the triggering rainfall. In terms of  
164 duration, DF occurrence is dominated by events with duration >24h, which account for  
165 ~82% of the DF occurrences, while in terms of rainfall accumulation DF events are  
166 distributed more uniformly with 25-30% of cases corresponding to each of the three  
167 highest classes (> 100 mm, 50-100 mm and 20-50 mm) and ~14% for the lowest class  
168 (<20 mm). Visual interpretation of the spatial pattern of rainfall properties (Fig. 3) shows  
169 that classes of rainfall and duration are rather mixed without revealing clustering of  
170 specific rainfall properties. Perhaps the only noticeable feature from Fig. 3 is that most of  
171 the DF events located in the northwestern part of the study region are generally  
172 associated with relatively low (<50 mm) rainfall accumulation. This is an indication of  
173 the link with the local climatic characteristics, with this portion of the study area being  
174 included in the dry internal alpine region, characterized by relatively low mean annual  
175 precipitation amounts.

### 176 **3.2 Seasonality of DF events**

177 Relationship between DF events and season is examined to analyze the importance of  
178 seasonality in a) the occurrence of DF events and b) the corresponding DF rainfall  
179 properties. Geographical distribution of the season of occurrence of the DF events is  
180 shown in Figure 4a, which reveals two important features. First, summer and fall season  
181 dominate DF occurrence in the region of study. Specifically, 49% of the DF occurred  
182 during summer and 43% during fall season (see Table 2 for more details). Second, there  
183 is a very distinct geographical separation between the two dominant seasons of DF  
184 occurrence. DFs in the northern part of the area are mainly occurring during the summer

185 while at the southern part, DFs occur predominantly during the fall season. In addition,  
186 examining the seasonal distribution of DF rainfall events (Table 2) shows that summer  
187 season is associated with 59% of the rainfall events while spring and fall seasons  
188 correspond almost equally to 16% each and winter to ~9%. Relating the seasonal  
189 distribution of the number of rainfall events with that of DF occurrences indicates clearly  
190 that rainfall events during fall season are associated with the highest (on average) DF  
191 numbers per event. Specifically, the ratio DF/event is 1.25(winter), 2.2 (spring), 5.4  
192 (summer) and 17.75 (fall).

193 To further investigate the relationship between seasonality and number of DFs triggered  
194 per rainfall event, we classified DF rainfall events according to the total number of DFs  
195 triggered and analyzed the seasonal distribution of each class. Five classes were  
196 considered that included rainfall events with total DF triggered equal to: 1 (class 1, 63  
197 events),  $1 < DF \leq 5$  (class 2, 35 events),  $5 < DF \leq 10$  (class 3, 13 event),  $10 < DF \leq 20$  (class 4,  
198 11 events) and  $DF > 20$  (class 5, 6 events). Examination of the results (Fig. 4b) shows that  
199 summer is clearly the dominant season in all classes. This is not surprising given that the  
200 greatest number of rainfall events is also associated with summer season. For the first  
201 class that involved events with only 1 DF occurrence, 60% of occurrences is almost  
202 uniformly distributed among winter, spring and fall and the rest ~40% corresponds to  
203 summer. There are no winter events for classes higher than class 2 suggesting that all  
204 winter events are associated with low number of DF occurrence. On the contrary, spring  
205 events are apparent for class 4, suggesting that spring events can be associated with the  
206 triggering of several DFs. Interestingly, the highest class ( $DF > 20$ ) is equally distributed  
207 between summer and fall season. Occurrence of a large number of DF-triggering rainfall  
208 events during summer is hypothesized as a result of mesoscale convective systems that  
209 although they have a relatively limited spatial extent, they are usually associated high  
210 intensities. On the other hand, rainfall events during fall season are commonly  
211 widespread systems covering a large spatial extent and are associated with moderate  
212 intensities but long durations and rather wet antecedent soil moisture conditions.

213 To examine the connection between rainfall climatology and DF seasonal spatial patterns  
214 observed in the region, we present in Figure 5 the mean annual rainfall map (Fig.5a) and  
215 a comparison of the contribution of summer and fall season (Fig.5b), during the study

216 period. As shown in Figure 5a, southern part receives most of rainfall (~1000-1200 mm),  
217 northeastern part receives ~600-900 mm while the northwestern part of the region  
218 receives significantly less rainfall (~400 mm), as a result of the shadowing effect posed  
219 by the mountainous range surrounding the area. Looking at the relative importance on the  
220 annual rainfall of summer versus fall season (Fig.5b), it is clear that rainfall in the  
221 northwestern part is dominated by summer season which is twice or more the fall season  
222 rainfall and accounts overall for ~50% of annual rainfall (results not shown). Therefore  
223 dominance of summer season in DF occurrence in this part of the region reflects in  
224 essence the overall dominance of summer season in rainfall climatology. However,  
225 results for the southern part are interestingly different in the sense that in this case, the  
226 contribution of summer and fall is almost equal (i.e. ratio close to 1) and account for  
227 ~30% (results not shown) of annual rainfall. This means that the “preference” of DF to  
228 occur during fall season cannot be explained by the overall rainfall climatology and  
229 should be therefore attributed to other factors like antecedent wetness conditions (i.e.  
230 being wetter in the fall) and/or to the interactions between hydrogeomorphologic  
231 conditions and rainfall event properties.

232 A further step in the seasonal analysis of DF is related to the seasonality of DF rainfall  
233 properties. Figure 6 reports the distribution (as boxplots) of DF rainfall accumulation and  
234 duration for the summer and fall seasons. The sample size for the DF cases of winter and  
235 spring (see Table 2) is considered rather limited (number of DF<50), to be able to derive  
236 statistical properties of the underlying distribution with an adequate degree of robustness  
237 and therefore results for these cases were omitted. Results show that rainfall  
238 characteristics of DF triggering events are significantly different between summer and  
239 fall season. Events during the summer are associated with lower rainfall accumulation  
240 and shorter duration while during the fall events are characterized by higher  
241 accumulations and longer durations. Specifically, average rainfall accumulation  
242 (duration) for summer events is equal to 44mm (48h), while for fall events is equal to  
243 128mm (98h). These results are in agreement with the explanation provided above  
244 regarding events of convective nature dominating summer rainfall and frontal systems  
245 associated with long-lived widespread systems occurring in the fall season. Therefore,

246 properties of DF triggering rainfall events follow the general seasonal characteristics of  
247 rainfall events in the region without exhibiting any other particular pattern.

### 248 **3.3 Debris flows distribution and weather circulation patterns**

249 Following the same methodological framework of section 3.2, we examine in this section  
250 the relationship of DF occurrence and corresponding triggering rainfall properties, with  
251 the weather circulation patterns. As it may be observed in Fig. 7, weather circulation  
252 patterns corresponding to Mixed, Zonal West and Meridional Southeast and South (SE,  
253 E) groups dominate DF occurrence in the region. In addition, visual inspection of Fig.7a  
254 reveals the clustering (i.e. geographical preference) of specific types. For example, the  
255 southern part of the study regions is associated to SE, E group while northwest and  
256 central east is associated to Mixed and Zonal West groups. Results regarding the  
257 connection between weather type and the different classes of rainfall events (see section  
258 3.2) are reported in Fig. 7b. Again, results show clearly that Zonal West, Mixed and SE,  
259 E circulation patterns are the most dominant ones, with Meridional North (N) and  
260 Northeast, East (NE, E) having an apparent but significantly less percentage of  
261 occurrence. Although the number of events included in class 5 is only six, thus not  
262 permitting statistically significant interpretation of results, nevertheless it is interesting to  
263 note that rainfall events that triggered the highest number of DF in the region and  
264 occurred during summer and fall season (see Fig.4b) are predominantly associated with  
265 weather circulation patterns (50% SE,E and ~17% N) that are much less frequent than  
266 Mixed (which corresponds to 33%) and Zonal West (0% occurrence) according to the  
267 climatology presented in Fig.2.

268 Examination of rainfall characteristics as a function of the weather circulation patterns  
269 (Fig.8) shows the variability of both rainfall accumulation and duration with weather  
270 type. On average, accumulation and duration increases consistently moving from Zonal  
271 West (38mm, 42h) and Mixed (37mm, 42h), to N (75mm, 59h), to SE,E (128mm, 99h).  
272 Note that due to sample size limitations, results in Fig.8 are presented for the four most  
273 dominant weather type groups.

274

### 275 3.4 DF rainfall thresholds

276 Results obtained from previous sections revealed strong dependencies between DF  
277 triggering rainfall properties with a) season and b) weather circulation patterns. This  
278 allow us to hypothesize that there is merit in classifying DF events according to these  
279 factors and identifying the DF rainfall thresholds separately for each case. This could  
280 potentially result in the development of a set of thresholds that can be used according to  
281 different conditions (e.g. depending on the weather type) thus providing a more accurate  
282 prediction in comparison to using a universal threshold.

283 Rainfall thresholds, used for predicting possible debris flow occurrence, identify critical  
284 rainfall condition by linking rainfall intensity (or accumulation) and duration (for a  
285 review see Guzzetti et al., 2007, 2008). In this study we considered a widely used model  
286 for the definition of the rainfall thresholds, which is the intensity-duration (*ID*) threshold  
287 commonly adopting the power-law form

$$I = \alpha D^{-\beta} \quad (1)$$

288 where  $I$  ( $\text{mm h}^{-1}$ ) is the mean intensity and  $D$  (h) is the duration of the DF triggering  
289 rainfall. The multiplier ( $\alpha$ ) and exponent ( $\beta$ ) parameters are constants and are estimated  
290 by fitting the power-law model to the empirical data. For the estimation of parameters  $\alpha$   
291 and  $\beta$  we applied the *frequentist* approach proposed by Brunetti et al., 2010. Note that the  
292 *frequentist* method allows identifying *ID* thresholds at different levels of exceedance  
293 probabilities (see for example Brunetti et al. 2010 and Peruccacci et al., 2012). In this  
294 work we adopted a 5% exceedance level, which means that the probability of a debris  
295 flow triggering rainfall event ( $I, D$  pair) to be under the estimated *ID* threshold is less  
296 than 5%.

297 To evaluate the significance of seasonal and weather type dependence of *ID* thresholds,  
298 we estimated the *ID* parameters from each DF sample corresponding to different season  
299 and weather circulation type. Note that in both cases, only the dominant seasons and  
300 weather types were examined. Also,  $I, D$  pairs used for the estimation of thresholds were  
301 filtered to remove values associated with  $I < 1 \text{ mm h}^{-1}$  and/or  $D < 2\text{h}$ , which are considered  
302 to fall within a range associated with high estimation uncertainty. Marra et al. 2014 has

303 shown that using  $I, D$  pairs below these thresholds may lead to unrealistic values of  $ID$   
304 parameters. Filtering and splitting the original DF sample (821 data points) according to  
305 season and weather type group introduces uncertainty in the  $ID$  estimation procedure due  
306 to the size of individual samples considered. To account for this effect, we applied the  
307 methodology developed by Peruccacci et al. (2012). Specifically, for each case,  $ID$   
308 estimation was repeated 1000 times on samples derived from the original population  
309 following the bootstrapping resampling technique (see Peruccacci et al. 2012 for more  
310 details). Results on the estimation of parameters  $\alpha$  and  $\beta$  and the uncertainty associated  
311 to sample size are summarized in Table 3 and are visualized in Fig.9 (for different  
312 seasons) and Fig. 10 (for different weather types).

313 Several conclusions can be drawn from these results. The estimated  $ID$  parameters for  
314 summer and fall differ mainly on parameter  $\alpha$ , with  $ID$  for fall being associated with  
315 higher value. The sampling uncertainty appears significant mostly for the  $\alpha$  parameter  
316 and is higher for fall. However, it can only partially explain the seasonal difference in  
317 parameter  $\alpha$ . Comparison of  $ID$  thresholds for different weather types shows that DF  
318 cases associated with Meridional North pattern, are characterized by significantly higher  
319 (than in all other weather types) values of both  $ID$  parameters. Results for Zonal West  
320 and Mixed patterns are associated with very low values for parameter  $\beta$  in comparison  
321 with the other cases but also with reference to other thresholds reported in literature (see  
322 Guzzetti et al., 2007). Despite the associated uncertainties due to sampling size, overall  
323 the results presented (Table 3, Fig.9 and Fig.10) show that classification of DF according  
324 to season or weather type can lead to considerably different thresholds. This has  
325 important implications for the operational use of the thresholds.

## 326 **4 Conclusions**

327 In this work, the seasonal and atmospheric circulation patterns of debris flows in the  
328 Eastern Italian Alps was examined. The study was focused on the Trentino-Alto Adige  
329 region and analysis was carried out over a ten years (2000-2009) period, for which a  
330 unique catalog of debris flow occurrences and hourly rain gauge precipitation was  
331 available. The principal conclusions derived are summarized below.

- 332 • The vast majority (92%) of debris flows occur during summer and fall season.  
333 Furthermore, the two dominant seasons exhibit a clear geographical preference,  
334 with summer and fall season dominating the northern and southern part  
335 respectively. Analysis of these results with respect to the general rainfall  
336 climatology in the region showed that dominance of summer season in DF  
337 occurrence at the northwestern part is expected since it accounts for 50% of  
338 annual rainfall and contributes twice the rainfall relative to fall season. However,  
339 rainfall during summer and fall season at the southern part has equal contribution  
340 (~30%), which suggests that dominance of DF occurrence during fall season at  
341 the southern part is probably controlled by other rainfall properties and/or other  
342 variables (e.g. higher antecedent soil moisture)
- 343 • Rainfall properties (accumulation and duration) derived for each individual debris  
344 flow location and from the closest available raingauge, exhibit a seasonal pattern  
345 as well. On average, summer events are associated with lower rainfall  
346 accumulation and shorter duration than fall events but with higher intensity.  
347 Essentially, this is a reflection of the general seasonal characteristics of rainfall in  
348 the region, where rainfall during summer is dominated by short duration  
349 convective systems, while during fall season widespread long-lived systems  
350 prevail (Borga et al., 2005).
- 351 • Weather circulation groups of Mixed, Zonal West and Meridional Southeast and  
352 South patterns dominate debris flow occurrences in the region. Debris flow  
353 triggering rainfall properties vary considerably with weather type and specifically,  
354 both duration and accumulation increase on average moving from Zonal West, to  
355 Mixed, to N and finally to SE,E.

356 Variability of rainfall properties with season and weather type was further examined in  
357 the context of *ID* thresholds used for the prediction of debris flow occurrence. Results  
358 revealed that there are indeed apparent differences in the *ID* thresholds estimated for each  
359 case (season or weather type). Although sampling size limitations introduce a  
360 considerable amount of uncertainty in the estimated thresholds, this alone cannot fully  
361 explain the observed differences. Therefore, results indicate that there is potentially merit



362 in the application of a classification scheme (according to season and/or circulation type)  
363 on debris flow event for improving accuracy of threshold-based prediction systems.

364

365 An important note that should be kept in mind when considering the results reported in  
366 this work regarding the derived rainfall properties and *ID* thresholds is that those depend  
367 on a) the identification of individual rainfall events and b) on the accuracy of rainfall  
368 estimates obtained from closest available gauges. Regarding the first point, we  
369 acknowledge that the use of an inter-event period of 24h may not always represent well  
370 the properties of the debris-flow triggering storms, especially in the case of short  
371 rainstorms spaced by few hours, and can therefore impact at some degree the derived  
372 values. We adopted the 24h threshold as a realistic value of a minimum period between  
373 consecutive events according to our experience and also following previous work  
374 (Nikolopoulos et al. 2014) to allow our results to be comparable with similar studies.  
375 However, more advanced procedures for the identification of triggering rainfall as  
376 recently proposed by Vessia et al. (2014) could be considered for further enhancing this  
377 type of analysis. On the second issue, which relates to the DF rainfall estimation from  
378 closest gauges, recent work on this topic (Nikolopoulos et al. 2014, Marra et al. 2014) has  
379 demonstrated clearly that gauge-based estimates of DF rainfall are largely  
380 underestimated, due to distance between closest gauge and DF location, and this results  
381 also in underestimation of *ID* thresholds. However, the current work focuses mostly on  
382 highlighting the relative differences of rainfall properties and subsequently of *ID*  
383 thresholds among different seasons/weather types and thus the absolute accuracy is not of  
384 focus. Therefore, we feel that the patterns portrayed regarding the seasonality and  
385 atmospheric circulation dependence hold despite the existence of bias in rainfall  
386 estimates.

## 387 **Acknowledgements**

388 This work is supported from EU FP7 Marie Curie Actions IEF project PIEF-GA-2011-  
389 302720 (HYLAND). We sincerely acknowledge Ripartizione Opere Idrauliche, and

390 Servizio Bacini Montani, of the Autonomous Province of Bolzano and Trento (Italy),  
391 respectively, for providing access to the archive of debris flows and for discussion on the  
392 results. The rain gauge data used in this work were provided by Ufficio Idrografico  
393 (Bolzano) and Meteotrentino (Trento).

394

395

## References

- 397 Borga, M., Stoffel, M., Marchi, L., Marra, F. and Jakob, M.: Hydrogeomorphic response  
398 to extreme rainfall in headwater systems: Flash floods and debris flows, *J Hydrol*, 518,  
399 Part B(0), 194–205, doi:10.1016/j.jhydrol.2014.05.022, 2014.
- 400 Borga, M., Vezzani, C. and Fontana, G. D.: Regional rainfall depth–duration–frequency  
401 equations for an alpine region, *Nat Hazards*, 36(1), 221–235, 2005.
- 402 Brunetti, M. T., Peruccacci, S., Rossi, M., Luciani, S., Valigi, D. and Guzzetti, F.:  
403 Rainfall thresholds for the possible occurrence of landslides in Italy, *Nat. Hazards Earth*  
404 *Syst. Sci.*, 10(3), 447–458, doi:10.5194/nhess-10-447-2010, 2010.
- 405 Dowling, C. and Santi, P.: Debris flows and their toll on human life: a global analysis of  
406 debris-flow fatalities from 1950 to 2011, *Nat Hazards*, 71(1), 203–227,  
407 doi:10.1007/s11069-013-0907-4, 2014.
- 408 Gestengabe, R.W. and Werner, P.C.: Katalog der Grosswetterlagen Europas (1881–  
409 2004) Nach Paul Hess Und Helmut Brezowsky. 6, Verbesserte und Ergänzte Auflage,  
410 PIK Report No. 100, Potsdam Institut Für Klimafolgenforschung, 153 pp, 2005 (in  
411 German).
- 412 Govi, M., Mortara, G., and Sorzana, P.F.: Eventi idrologici e frane, *Geologia Applicata e*  
413 *Idrogeologia*, 20(1), 359-375, 1985 (In Italian).
- 414 Guzzetti, F., Peruccacci, S., Rossi, M. and Stark, C.: The rainfall intensity–duration  
415 control of shallow landslides and debris flows: an update, *Landslides*, 5(1), 3–17–17,  
416 doi:10.1007/s10346-007-0112-1, 2008.
- 417 Guzzetti, F., Peruccacci, S., Rossi, M. and Stark, C. P.: Rainfall thresholds for the  
418 initiation of landslides in central and southern Europe, *Meteorology and Atmospheric*  
419 *Physics*, 98(3-4), 239–267–267, doi:10.1007/s00703-007-0262-7, 2007.
- 420 Hess P, Brezowsky H (1952) Katalog der Grosswetterlagen Europas. Berichte des  
421 Deutschen Wetterdienstes in der US-Zone, 33
- 422 Hess P, Brezowsky H (1969) Katalog der Grosswetterlagen Europas, 2. neu bearbeitete  
423 und ergaanzte Aufl. Berichte des Deutschen Wetterdienstes 113. Offenbach am Main
- 424 Hess P, Brezowsky H (1977) Katalog der Grosswetterlagen Europas 1881–1976, 3.  
425 verbesserte und ergaanzte Aufl. Berichte des Deutschen Wetterdienstes 113. Offenbach  
426 am Main
- 427 James, P. M.: An objective classification method for Hess and Brezowsky  
428 Grosswetterlagen over Europe, *Theor. Appl. Climatol.*, 88(1-2), 17–42,  
429 doi:10.1007/s00704-006-0239-3, 2007.

- 430 Kysely, J. and Huth, R.: Changes in atmospheric circulation over Europe detected by  
431 objective and subjective methods, *Theor. Appl. Climatol.*, 85(1-2), 19–36,  
432 doi:10.1007/s00704-005-0164-x, 2006.
- 433 Marra, F., Nikolopoulos, E. I., Creutin, J.-D. and Borga, M.: Radar rainfall estimation for  
434 the identification of debris-flow occurrence thresholds, *J Hydrol*, 519, Part B(0), 1607–  
435 1619, doi:10.1016/j.jhydrol.2014.09.039, 2014.
- 436 Mei, Y., Anagnostou, E. N., Nikolopoulos, E. I. and Borga, M.: Error Analysis of  
437 Satellite Precipitation Products in Mountainous Basins, *J. Hydrometeorol.*, 15(5), 1778–  
438 1793, doi:10.1175/JHM-D-13-0194.1, 2014.
- 439 Nikolopoulos, E. I., Crema, S., Marchi, L., Marra, F., Guzzetti, F. and Borga, M.: Impact  
440 of uncertainty in rainfall estimation on the identification of rainfall thresholds for debris  
441 flow occurrence, *Geomorphology*, 221, 286–297, doi:10.1016/j.geomorph.2014.06.015,  
442 2014.
- 443 Norbiato, D., Borga, M., Merz, R., Blöschl, G. and Carton, A.: Controls on event runoff  
444 coefficients in the eastern Italian Alps, *J Hydrol*, 375(3-4), 312–325,  
445 doi:10.1016/j.jhydrol.2009.06.044, 2009.
- 446 Parajka, J., Kohnová, S., Bálint, G., Barbuc, M., Borga, M., Claps, P., Cheval, S.,  
447 Dumitrescu, A., Gaume, E., Hlavčová, K., Merz, R., Pfaundler, M., Stancalie, G.,  
448 Szolgay, J. and Blöschl, G.: Seasonal characteristics of flood regimes across the Alpine  
449 Carpathian range, *J Hydrol*, 394(1-2), 78–89, doi:10.1016/j.jhydrol.2010.05.015, 2010.
- 450 Peruccacci, S., Brunetti, M. T., Luciani, S., Vennari, C. and Guzzetti, F.: Lithological and  
451 seasonal control on rainfall thresholds for the possible initiation of landslides in central  
452 Italy, *Geomorphology*, 139-140(C), 79–90, doi:10.1016/j.geomorph.2011.10.005, 2012.
- 453 Petley, D.: Global patterns of loss of life from landslides, *Geology*, 40(10), 927–930,  
454 doi:10.1130/G33217.1, 2012.
- 455 Planchon, O., Quénol, H., Dupont, N. and Corgne, S.: Application of the Hess-  
456 Brezowsky classification to the identification of weather patterns causing heavy winter  
457 rainfall in Brittany (France), *Nat Hazard Earth Sys*, 9(4), 1161–1173, 2009.
- 458 Salvati, P., Bianchi, C., Rossi, M. and Guzzetti, F.: Societal landslide and flood risk in  
459 Italy, *Nat. Hazards Earth Syst. Sci.*, 10(3), 465–483, doi:10.5194/nhess-10-465-2010,  
460 2010.
- 461 Schneuwly-Bollschweiler, M. and Stoffel, M.: Hydrometeorological triggers of  
462 periglacial debris flows in the Zermatt valley (Switzerland) since 1864, *J. Geophys. Res.*,  
463 117(F2), F02033, doi:10.1029/2011JF002262, 2012.
- 464 Stoffel, M., Tiranti, D. and Huggel, C.: Climate change impacts on mass movements —  
465 Case studies from the European Alps, *Science of The Total Environment*, 493, 1255–  
466 1266, doi:10.1016/j.scitotenv.2014.02.102, 2014.

467 Toreti, A., Schneuwly-Bollschweiler, M., Stoffel, M. and Luterbacher, J.: Atmospheric  
468 Forcing of Debris Flows in the Southern Swiss Alps, *J. Appl. Meteor. Climatol.*, 52(7),  
469 1554–1560, doi:10.1175/JAMC-D-13-077.1, 2013.

470 Turkington, T., Ettema, J., Van Westen, C. J. and Breinl, K.: Empirical atmospheric  
471 thresholds for debris flows and flash floods in the southern French Alps, *Nat. Hazards*  
472 *Earth Syst. Sci.*, 14(6), 1517–1530 [online] Available from: [http://www.nat-hazards-](http://www.nat-hazards-earth-syst-sci-discuss.net/2/757/2014/nhessd-2-757-2014.pdf)  
473 [earth-syst-sci-discuss.net/2/757/2014/nhessd-2-757-2014.pdf](http://www.nat-hazards-earth-syst-sci-discuss.net/2/757/2014/nhessd-2-757-2014.pdf), 2014.

474 Vennari, C., Gariano, S. L., Antronico, L., Brunetti, M. T., Iovine, G., Peruccacci, S.,  
475 Terranova, O. and Guzzetti, F.: Rainfall thresholds for shallow landslide occurrence in  
476 Calabria, southern Italy, *Nat. Hazards Earth Syst. Sci.*, 14(2), 317–330,  
477 doi:10.5194/nhess-14-317-2014, 2014.

478 Vessia, G., Parise, M., Brunetti, M. T., Peruccacci, S., Rossi, M., Vennari, C. and  
479 Guzzetti, F.: Automated reconstruction of rainfall events responsible for shallow  
480 landslides, *Nat. Hazards Earth Syst. Sci.*, 14(9), 2399–2408, 2014.

481

482 Table 1. Groups of weather circulation pattern according to Grosswetterlagen  
483 classification scheme.

GWL group	GWL type (see Gestengabe and Werner (2005))
Zonal West	WA, WZ, WS, WW
Mixed	SWA, SWZ, NWA, NWZ, HM, BM
Mixed Central Europe (CE)	TM
Meridional North (N)	NA, NZ, HNA, HNZ, HB, TRM
Meridional Northeast and East (NE, E)	NEA, NEZ, HFA, HFZ, HNFA, HNFZ
Meridional Southeast and South (SE, E)	SEA, SEZ, SA, SZ, TB, TRW

484

485

486 Table 2. Number of debris flows and individual rainfall events per season and weather  
487 type group. Results are reported also as percentages in the parenthesis.

<b>Season</b>	<b>Number of DF (total=821)</b>	<b>Number of rainfall events (total=128)</b>
Winter	15 (2%)	12 (9%)
Spring	46 (6%)	21 (16%)
Summer	405 (49%)	75 (59%)
Fall	355 (43%)	20 (16%)
<b>GWL group</b>		
Zonal West	95 (12%)	30 (23%)
Mixed	179 (22%)	44 (34%)
CE	7 (1%)	4 (3%)
N	86 (10%)	14 (12%)
NE, E	55 (7%)	9 (7%)
SE,E	399 (49%)	27 (21%)

488

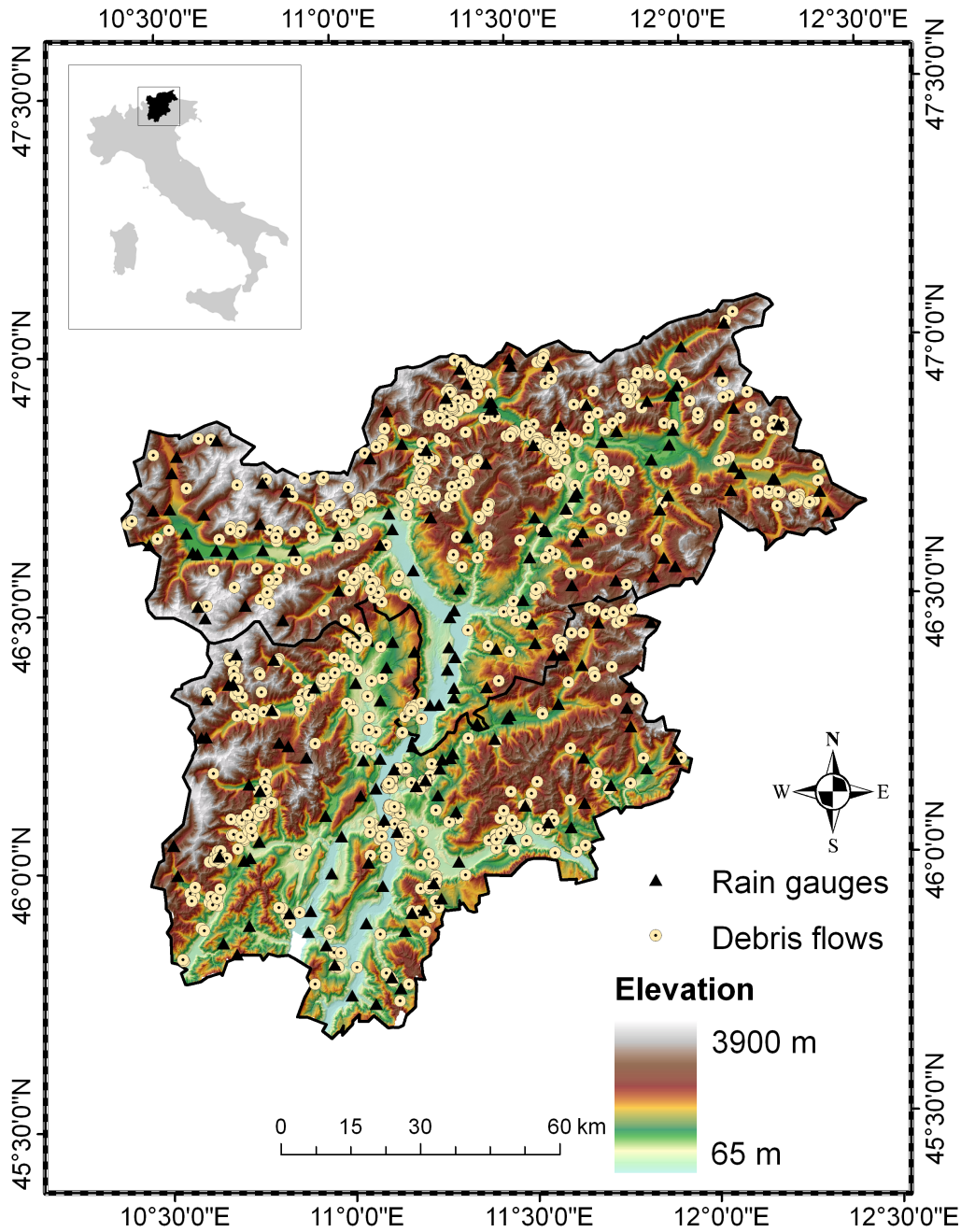
489

490 Table 3. Estimated *ID* parameters ( $\alpha, \beta$ ) from original sample and their corresponding  
 491 mean ( $\mu$ ) and standard deviation ( $\sigma$ ) derived from the resampling exercise.

<b>Season</b>	$\alpha$	$\mu_\alpha (\sigma_\alpha)$	$\beta$	$\mu_\beta (\sigma_\beta)$
Summer	2.63	2.68(0.40)	0.30	0.31(0.04)
Fall	3.64	3.75(0.76)	0.28	0.28(0.04)
<b>GWL group</b>				
Zonal West	2.22	2.42(0.74)	0.34	0.34(0.10)
Mixed	1.41	1.45(0.32)	0.12	0.11(0.06)
N	6.10	6.43(2.01)	0.47	0.46(0.08)
SE, E	1.92	2.00 (0.49)	0.14	0.14(0.05)

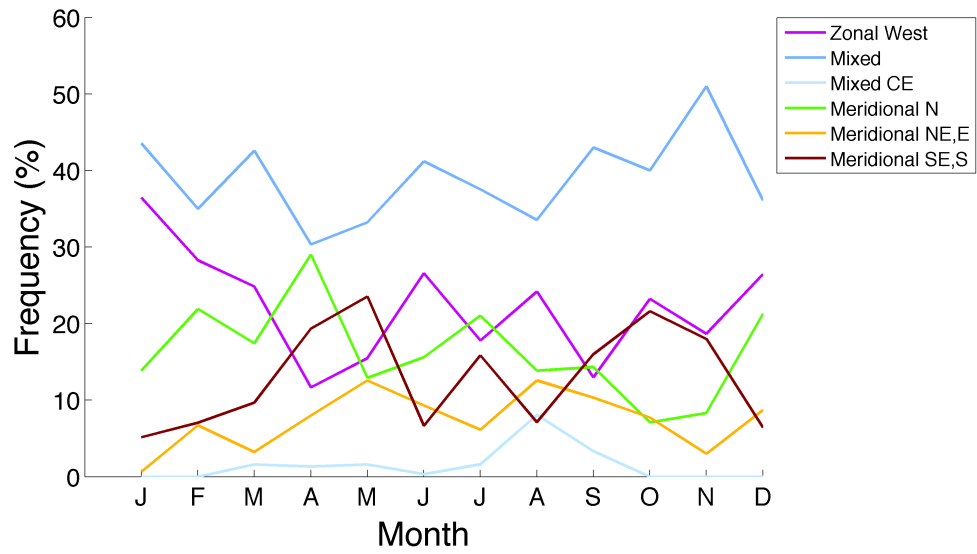
492  
 493





494  
 495 Fig.1. Map of the Trentino - Alto Adige region. Shades of color show terrain elevation.  
 496 Triangles and circles show respectively the location of rain gauges and debris flows  
 497 involved in current study.

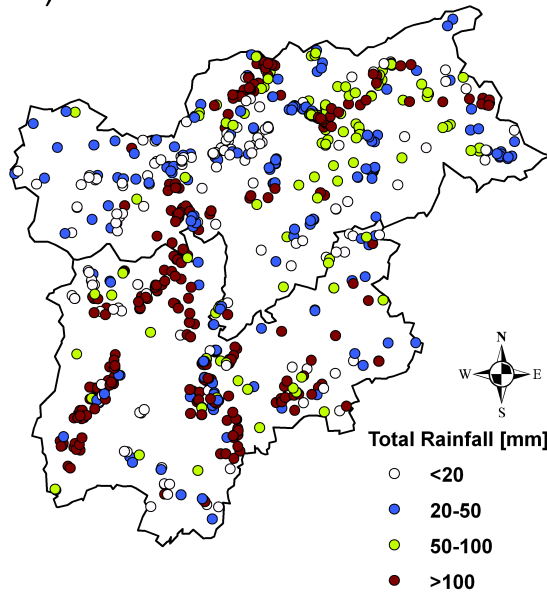
498  
 499



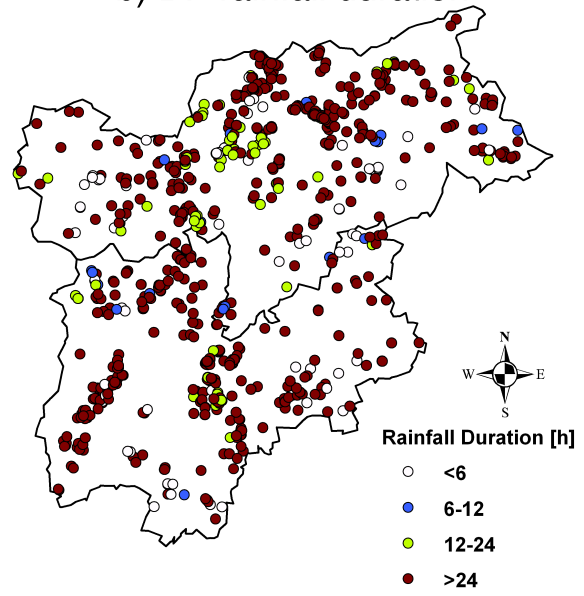
500  
 501  
 502  
 503  
 504  
 505  
 506

Fig.2 : Frequency of occurrence of weather circulation patterns classified in the Groswwetterlagen catalogue in the period 2000–2009.

a) DF-rainfall accumulation



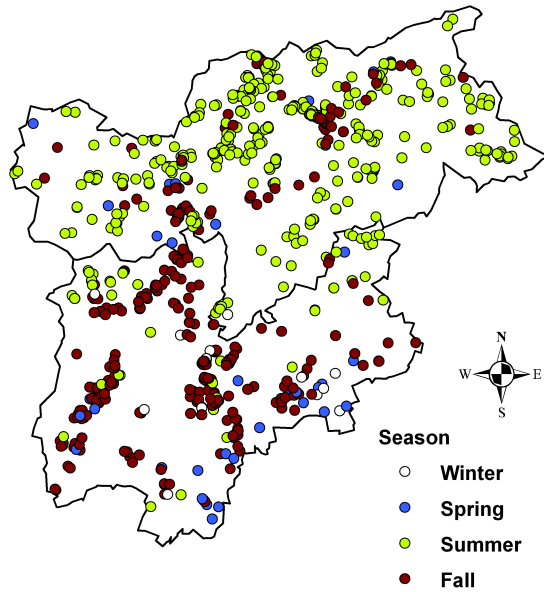
b) DF-rainfall duration



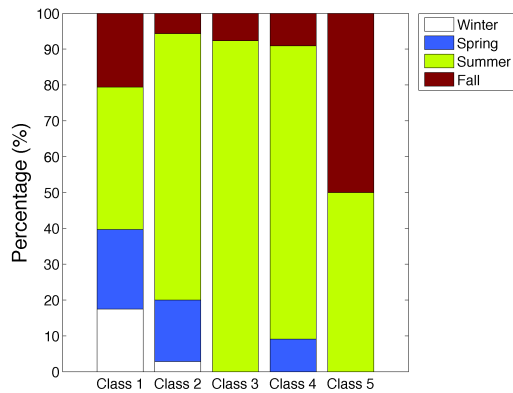
507  
508  
509

Fig.3 Map showing spatial distribution of DF rainfall a) accumulation and b) duration.

a) Spatial distribution of DF season



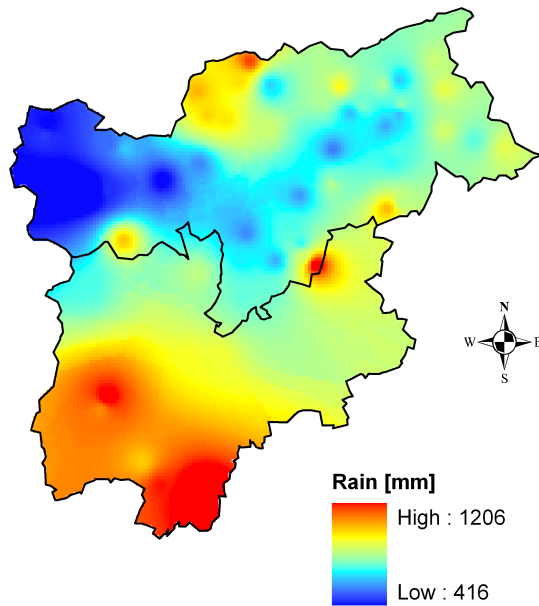
b) Seasonal contribution to DF classes



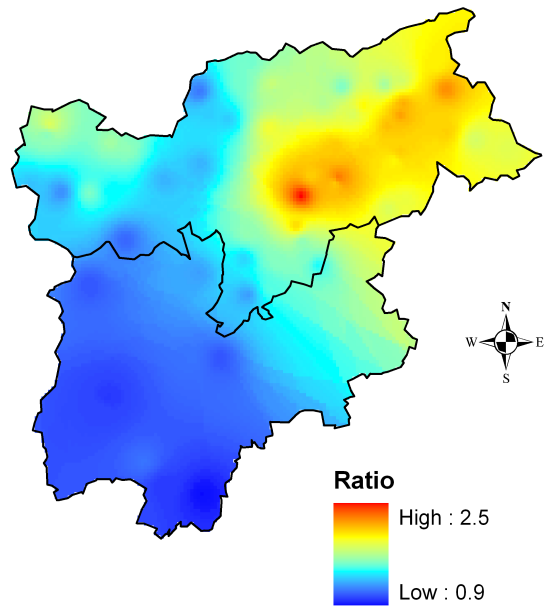
510  
511  
512  
513  
514  
515  
516  
517

Fig.4 Seasonality of DF occurrence: a) Map showing spatial distribution of DF locations color coded according to season of occurrence, b) Correspondence between season and percentage of DF rainfall events, classified according to number of triggered DF. See section 3.2 for definition of classes.

a) Average annual rain



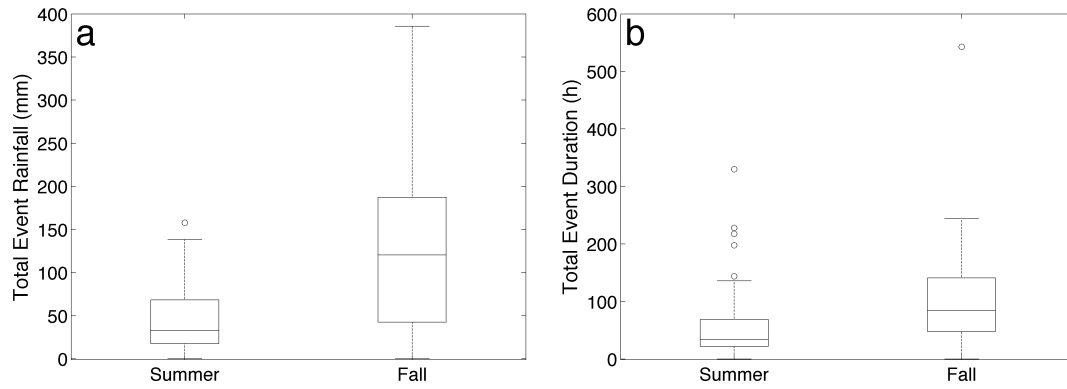
b) Summer/Fall contribution



518  
519  
520  
521  
522  
523  
524

Fig.5. Annual rainfall climatology and seasonal contribution. Average annual rainfall derived from available observations (a) and ratio of summer/fall contribution to annual rainfall (b). Note that available rain gauge observations were spatially interpolated using inverse distance weighted technique to produce the spatial maps shown.

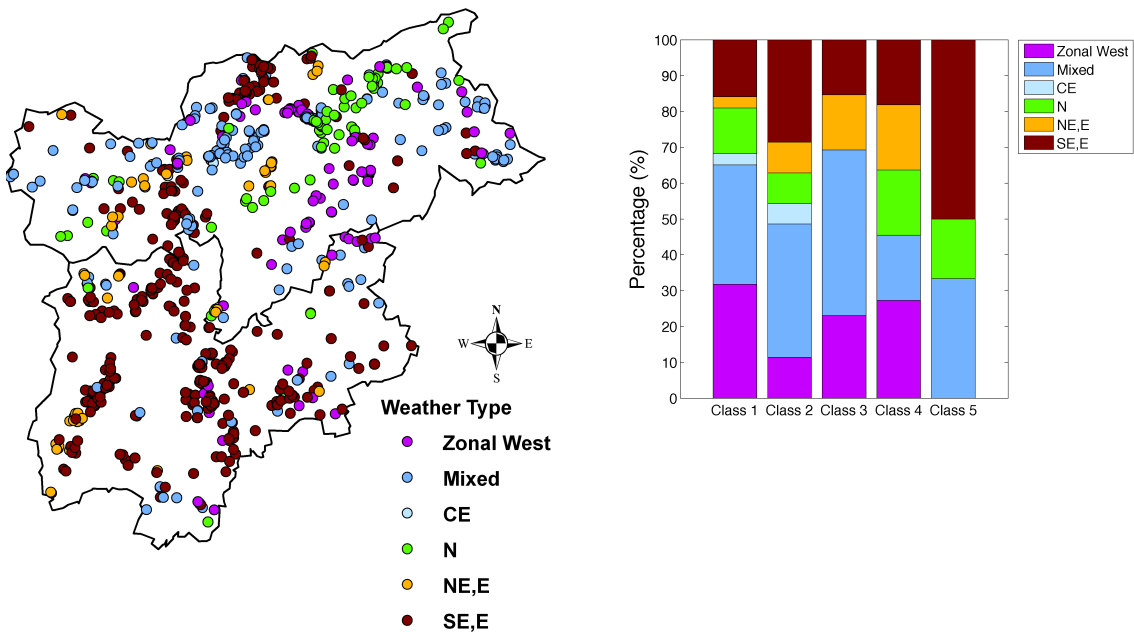
525  
526



527  
528  
529  
530  
531  
532  
533  
534

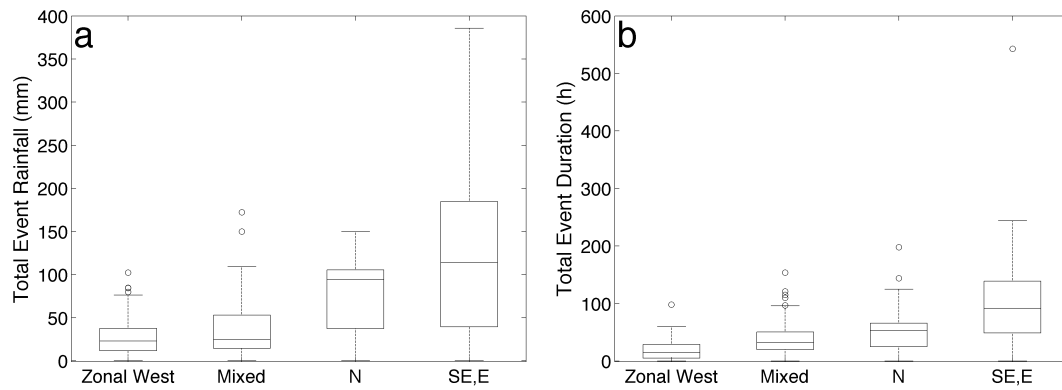
Fig.6. Box-plots of DF rainfall accumulation (a) and duration (b) for summer and fall season. Circles correspond to outliers of the distribution (identified as greater than 1.5 times the inter-quartile range).

a) Spatial distribution of DF weather type b) Weather type contribution to DF classes



535  
536  
537  
538  
539  
540  
541

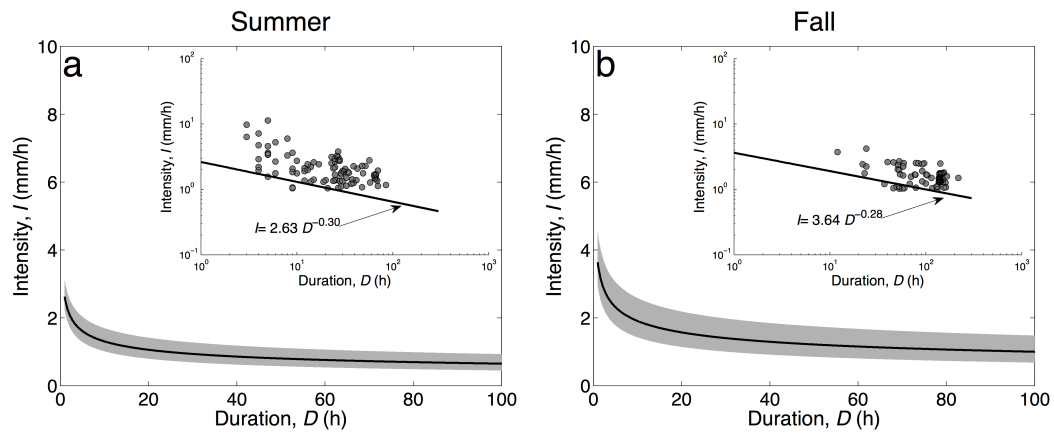
Fig.7 Weather type dependence of DF occurrence: a) Map showing spatial distribution of DF locations color coded according to weather type group, b) Correspondence between weather type and percentage of DF rainfall events, classified according to number of triggered DF. See section 3.2 for definition of classes.



542  
 543  
 544  
 545  
 546  
 547

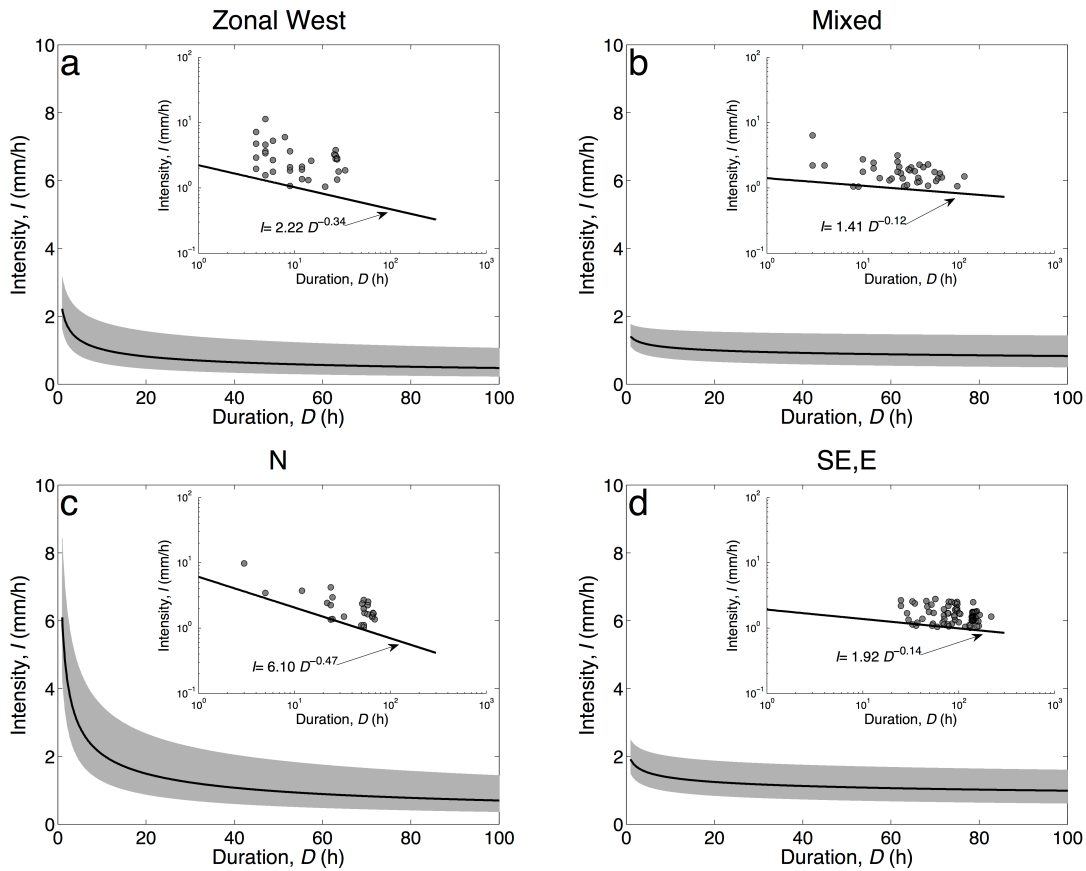
Fig.8. Box-plots of DF rainfall accumulation (a) and duration (b) of DF events associated with Zonal West, Mixed, Meridional North and Meridional Southeast and South weather type groups (Table 1). Circles correspond to outliers of the distribution (identified as greater than 1.5 times the inter-quartile range).





548  
 549  
 550  
 551  
 552  
 553  
 554  
 555

Fig.9. Intensity-Duration thresholds estimated for a) summer and b) fall seasons. Black line corresponds to  $ID$  thresholds estimated from corresponding DF samples. Grey shade denotes the uncertainty bounds equal to the mean  $\pm 1$  standard deviation of the parameter values obtained from the resampling exercise (see Table 3).



557  
 558  
 559  
 560  
 561  
 562  
 563  
 564  
 565  
 566  
 567

Fig.10. Intensity-Duration thresholds estimated for a) Zonal West, b) Mixed, c) Meridional North and d) Meridional Southeast and South weather type groups. Black line corresponds to ID thresholds estimated from corresponding DF samples. Grey shade denotes the uncertainty bounds equal to the mean  $\pm$  1 standard deviation of the parameter values obtained from the resampling exercise (see Table 3).